20 July 2001

ELSEVIER

Chemical Physics Letters 342 (2001) 571–577

CHEMICAL PHYSICS LETTERS

www.elsevier.com/locate/cplett

One-photon UV detrapping of the hydrated electron

Dong Hee Son, Patanjali Kambhampati, Tak W. Kee, Paul F. Barbara *

Department of Chemistry and Biochemistry, University of Texas, Welch Hall, 24th and Speedway, Austin, TX 78712, USA

Received 22 December 2000; in final form 17 January 2001

Abstract

Direct 1-photon excitation of the hydrated electron from the ground state to the conduction band is achieved with 400 nm excitation. This provides a unique method for investigating the femtosecond dynamics and spectroscopy of the conduction band hydrated electron without interference from other states. The assignment of the 400 nm excited state to the conduction band is supported by the observation of >35 Å spatial migration of the hydrated electron, as manifested in complete supression of geminate recombination. Similar dynamics and electron scavenging yields are observed for the 400 nm state and that produced by 2-photon 800 nm excitation. © 2001 Elsevier Science B.V. All rights reserved.

1. Introduction

The equilibrated form (e_{eq}) of the excess electron in water (the hydrated electron) is a spherical s-like state, that is localized, trapped and solvated in a solvent cavity [1,2]. The cavity is immediately surrounded by ~6 H_2O molecules. The radius from the center of the cavity to the oxygen atom center of H_2O is ~2.5 Å. The rigorous understanding of the spectroscopy and dynamics of e_{eq} is critical to the development of many fields, including the radiation-chemistry [3,4], -biology [5,6] and -physics [6] of water and aqueous solutions; the investigation of the ultrafast dynamics of coupled mixed electron/nuclear degrees-of-freedom systems [7,8]; and the investigation of electron localization/delocalization in condensed systems. In particular, the investigation of the hydrated electron relaxation on the femtosecond time scale has been extensively investigated [9–16]. The main peak in the e_{eq} absorption spectrum (Fig. 1) has been assigned to an s → p transition between the localized s ground state and three non-degenerate p-like sub-states [17]. The p-states are localized and trapped in the same solvent cavity as the original e_{eq} [18]. A molecular-level description of the s → p transition is available in electronic structure calculations on the hydrated electron coupled to a molecular dynamics description of the surrounding water [8,17]. The optically excited p-state is found to be significantly larger than its parent s-state, as shown schematically in Fig. 1. The major contribution to the oscillator strength (>90%) is assigned to the s → p transition, with the remainder due to the fourth and higher excited states. Finally, the simulations indicate that the extraordinarily large width of the transition is due to both the p-state splitting and a distribution of solvent environments (cavity size and water orientation).

This Letter is concerned with optically excited states of the hydrated electron that are higher in

* Corresponding author. Fax: +1-512-471-3389.
E-mail address: p.barbara@mail.utexas.edu (P.F. Barbara).

0009-2614/01/$ - see front matter © 2001 Elsevier Science B.V. All rights reserved.
PII: S0009-2614(01)00167-1

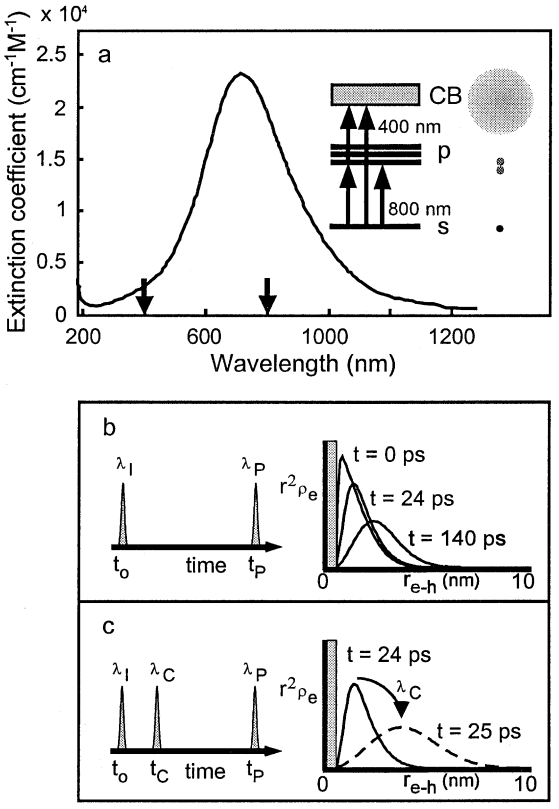

Fig. 1. (a) Absorption spectrum and electronic energy level diagram of the hydrated electron. The arrows in the spectrum indicate the excitation wavelengths in the present experiment, which also corresponds to the excitation process indicated in the energy level diagram in the figure. The relative sizes (from [29,30]) of the hydrated electron in the various states are also shown in the figure. (b) and (c) Schematic illustration of optical control of the spatial distribution and geminate recombination of the hydrated electron. The sequence consists of ionization (266 nm), control (800 and 400 nm), and probe (650 nm) pulses. In panel b, the ionization pulse produces an initial distribution of e_{eq}/hole pairs and the probe pulse monitors the geminate recombination. In panel c, an additional control pulse spatially alters the e_{eq}/hole pair distribution suppressing the geminate recombination process.

energy than the three p-states. Simulations have shown that fourth and higher states are significantly delocalized on the distance scale of molecuar dynamics simulation (15 Å) [19]. These upper states have been interpreted as being continuum or conduction-band-like (Fig. 1). The first experimental evidence to support this hypothesis has recently been published by this laboratory [18]. The spatial extent of the optically excited states of the hydrated electron was monitored indirectly by using the geminate recombination of a photoionization produced e_{eq}/hole pair as a 'ruler'. As shown in Fig. 1b,c, the new 3-pulse experiment is an elaboration of the well-known 2-pulse photoionization/probe experiment. A typical example of the 2-pulse photoionization experiment is the 2-photon 266 nm photoionization of water. The femtosecond photoionization pulse induces 'below conduction band' electron ejection from water to a nearby pre-existing quasi-localized state in water [20–23]. Within ~1 ps after photoionization (i) the excess electrons relax to an equilibrated ground state and (ii) the initial H_2O^+ hole fragments to nearby H_3O^+ and OH radical species [24,25]. Due to the nature of the initial photoionization process with 2-photon 266 nm ionization, there is a Gaussian distribution of e_{eq}/hole pair separations (r_{e-h}) with a σ of 12 Å [26,27]. As time evolves the spatial distribution and concentration of e_{eq} evolve due to simultaneous translational diffusion and geminate recombination of closely spaced e_{eq}/hole pair. The fraction of surviving electron as a function of time (the survival dynamics, $S(t)$) is typically monitored over hundreds of picoseconds by a probe pulse in resonance with the $s \rightarrow p$ transition of e_{eq}. $S(t)$ can be analyzed in terms of a diffusion model (that is modified to include geminate recombination) in order to determine the inital width (σ) of the distribution of e_{eq}/hole separation [26].

The new 3-pulse experiment (Fig. 1c) includes an additional control pulse during the evolution period, e.g. $t = 24$ ps. The purpose of the control pulse is to 'test' the extent of delocalization of specific excited states of e_{eq} by determinng whether excitation and subsequent relaxation of the specific states alter the r_{e-h} distribution. In particular, it was recently shown that 2-photon excitation of e_{eq} at 800 nm to the conduction band (e_{CB}) induces an electron migration of >35 Å [18]. The sequence of events in the 3-pulse experiment with 2-photon 800 nm excitation is as follows:

$$e_{eq}(r_A) \overset{800\text{ nm}}{\rightarrow} \overset{800\text{ nm}}{\rightarrow} e_{CB} \overset{\text{relax at } \sim 1\text{ ps}}{\rightarrow} e_{eq}(r_B). \quad (1)$$

Here r_A and r_B are the positions of the electron before and after the 2-photon excitation. The alteration in the r_{e-h} distribution was monitored indirectly through the alteration of $S(t)$ due to the control pulse. Two-photon excitation of e_{eq} to form the conduction band state was observed to completely suppress geminate recombination [18]. It was observed that r_B is on average different from r_A by >35 Å. In contrast to the 2-photon 800 nm excitation, 1-photon excitation of e_{eq} does not significantly alter the r_{e-h} spatial distribution, and an unaltered $S(t)$ curve was observed. Hence we continue the investigation of 1-photon control pulse alteration of geminate recombination by using 400 nm control pulse, as shown in Fig. 1. While this process is energetically equivalent to 2-photon 800 nm conduction band preparation experiment, the experiments are different since the 2-photon experiment involves a $(1 + 1)$ excitation process in which the first photon is resonant with the $s \rightarrow p$ transition and the second photon excites the $p \rightarrow CB$ transitions. The direct excitation process with a 400 nm photon, incontrast, is simpler allowing for a direct connection to the 1-photon absorption spectrum (Fig. 1). Furthermore, the ability to produce a conduction band electron by single photon excitation with a 400 nm femtosecond pulse is shown in this Letter to be a powerful new approach for the investigation of the relaxation dynamics of the conduction band electron. This work is related to an earlier report of conduction band 1-photon detrapping with 300 nm excitation [28]. These measurements did not, however, deal with supressed geminate recombination. The earlier work also had insufficient time resolution to distinguish the different dynamics of the p-state and the conduction band reported herein.

In addition to the investigation of the ability of 400 nm excitation of e_{eq} to suppress geminate recombination, this paper also investigates the reaction of the 400 nm produced excited state with NO_3^-, an electron scavenger. Recent papers from this laboratory have shown that the p-state and conduction band electrons have different scavenging yields, allowing for an additional diagnostic for the assignment (CB or p-state) of the 400 nm excited state [29,30].

2. Experimental methods

The laser system used in these experiments is composed of a home built Kerr lens mode locked Ti:sapphire oscillator pumped by a Nd:YVO_4 laser and a Ti:sapphire multipass amplifier pumped by Nd:YLF laser. A detailed description of the laser sytem can be found elsewhere [12]. Briefly, <20 fs pulses centered at 800 nm and generated from the oscillator, were subsequently stretched and amplified to give <35 fs, 0.4 mJ pulses at 1 kHz after compression. The amplified femtosecond laser beam was divided into four beams. The first and second beam were used to generate the 266 nm photoionization pulses. The first beam was used to produce the second harmonic of the laser at 400 nm in a BBO crystal and then this light was mixed with the second beam of 800 nm light to produce the 266 nm pulse in a BBO crystal. The third beam of fundamental 800 nm light was used for the control pulse. For the 400 nm control pulse experiments it was doubled in a BBO crystal. The fourth beam of fundamental 800 nm light was used to produce white light continuum in a sapphire crystal. The continuum was used to probe the transient optical density of the hydrated electron after filtering and compensation for optical dispersion in a fused silica prism pair. The instrument response function for photoionization/probe experiment was ~100 fs FWHM. For the photoionization/control/probe configuration, the cross-correlation time between the probe and the control pulse was 50 and 120 fs for 800 and 400 nm control pulses, respectively. The sample solutions were continuously flowed through a 300 μm jet nozzle to avoid repeated exposure of the same region of the sample to the laser pulses.

3. Results and discussion

The 2-photon 266 nm, pump–probe photoionization dynamics of water is shown in Fig. 2a (solid line). The probe pulse ($\lambda = 650$ nm) monitors the time-dependent concentration of e_{eq}. The transient optical density reflects the survival dynamics of e_{eq} associated with the geminate recombination process, as described in Section 1 and

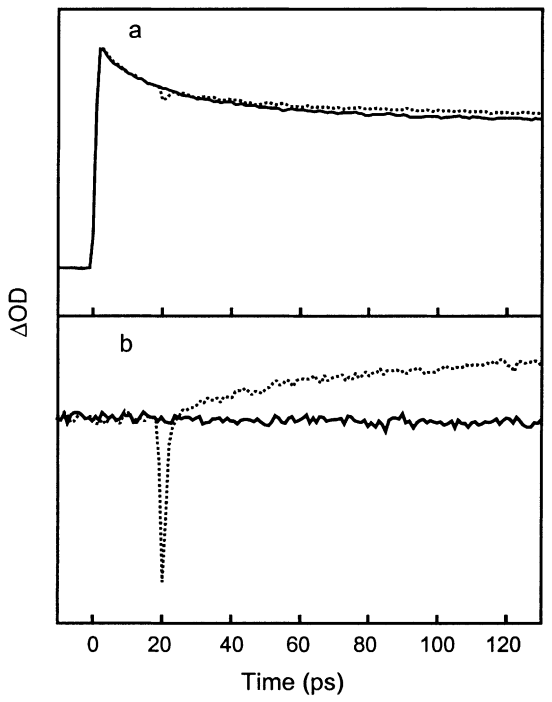

Fig. 2. Time evolution of the absorption of the hydrated electron generated by 266 nm multiphoton ionization. (a) Decay kinetics of the hydrated electron absorption due to the geminate recombination of e_{eq}/hole pair with (dotted line) and without (solid line) 400 nm control pulse. (b) The effect of control pulse on the geminate recombination kinetics is shown by chopping the control pulse and synchronously detecting the pulse-on minus pulse-off absorption. The baseline is for the same type of experiment with the 400 nm control pulse blocked but the photoionization pulse present.

elsewhere [18,26,27]. The addition of 400 nm control pulse at $t = 24$ ps induces a bleach at $t = 24$ ps due to ground state depletion. This is followed by a rapid relaxation (see dotted line in Fig. 2a). At longer times a portion of the geminate recombination is suppressed due to the 400 nm control pulse excitation. The altered dynamics due to the control pulse is especially apparent in data recorded with 'chopping' of the 400 nm pulse and synchronous detection of the e_{eq} absorption (dotted line in Fig. 2b). The suppressed geminate recombination is well above the detection limit or baseline of the spectrometer, which is reflected in the solid line in Fig. 2b. The baseline is a synchronously detected signal with the 400 nm control pulse blocked, but with the 266 nm signal still impinged on the sample. In addition, no signal is observed due to multiphoton ionization of water by the 400 nm pulses, which is too weak to induce the required 3-photon ionization [27,30]. The shape of the suppressed geminate recombination dynamics (Fig. 2b) is experimentally indistinguishable from the shape of the survival dynamics in the absence of the control pulse, although the sign is opposite. This behavior has been shown (in the case of 2-photon 800 nm suppression) to indicate that the excited state produced by the control pulse has a migration length >35 Å [30]. Thus, the suppressed geminate recombination data demonstrate that the 400 nm pulse produces a conduction band-like electron.

A 3-pulse pump–probe transient with 400 nm chopping and finer time steps is displayed in Fig. 3a (dotted line). The time axis has been shifted to

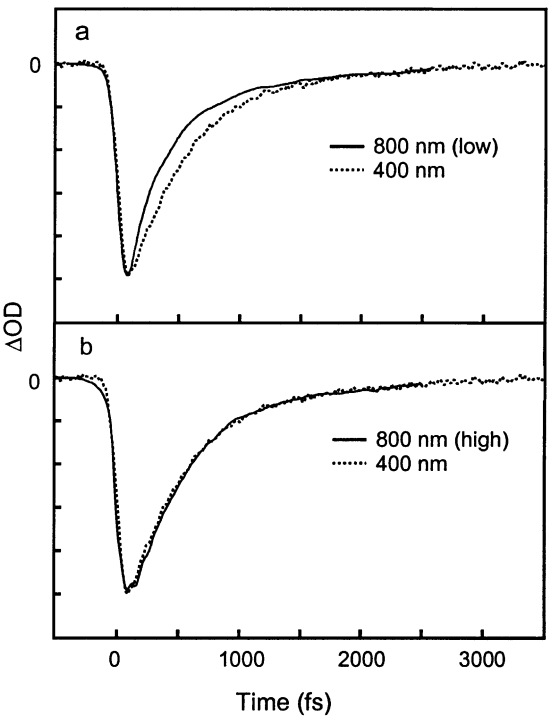

Fig. 3. Comparison of the pump–probe data of the hydrated electron at two different pump wavelengths 800 nm (solid line) and 400 nm (dotted line). Probe wavelength is 650 nm. The recovery of the ground state absorption with 400 nm pump is (a) slower compared to low intensity 800 nm pump, but (b) identical to high intensity 800 nm pump.

place that $t = 0$ point at the peak arrival time at the 400 nm control pulse. The suppressed geminate recombination that is apparent in Fig. 2 is too slow to observe in Fig. 3, which is over a smaller time region. At the probe wavelength (650 nm) the transient signal reflects ground state depletion of the e_{eq}, followed by electronic and solvent relaxation, which repopulates e_{eq}. The complete recovery of the signal within experimental error (3%) demonstrates that 400 nm excited electrons are not consumed by a chemical reaction with the solvent. The maximum bleach signal varies linearly with the pulse energy over the investigated range, consistent with a small degree of saturation of the transition and only single 400 nm photon excitation.

Fig. 4 plots the percent suppression of geminate recombination vs. the percent depletion of e_{eq} ground state population. For 400 nm excitation (circle points in Fig. 4) the linear behavior with a slope close to unity strongly demonstrates that of e_{eq} leads to a conduction band electron with a unity quantum yield. It is interesting to compare the data for 400 nm excitation to that for 800 nm excitation (square points in Fig. 4). The data with 800 nm excitation has a quadratic dependence on fractional bleach at low pulse energy indicating that 1-photon excitation at 800 nm does not suppress geminate recombination, but 2-photon excitation does suppress recombination. This implies that the 2-photon 800 nm excitation process and the 1-photon 400 nm excitation produce similar excited states.

Fig. 4. Fractional photo-induced suppression of the geminate recombination of the e_{eq}/hole pair generated by the photoionization of water. Wavelengths of the control pulses are 400 nm (circle) and 800 nm (square).

The similarity of the 2-photon 800 nm excitation process and the 1-photon 400 nm excitation process is supported by the data in Fig. 3b. The pump–probe transients recorded under the 1-photon 400 nm and 2-photon 800 nm conditions are nearly identical within experimental error (the 800 nm data in Fig. 3 have been slightly temporally broadened by convolution with a 150 fs Gaussian in order to correct for the longer pulse width of the 400 nm control pulse). In contrast to the similarity of the transients in Fig. 3b, the transients in Fig. 3a are clearly distinguishable. Here the transient due to 1-photon 800 nm excitation, which produces a p-state, relaxes significantly faster than the conduction band transient produced 1-photon 400 nm excitation.

We assign the difference between the relaxation dynamics in Fig. 3a to the identity of the excited state (conduction band vs. p-state) rather than simply the photon energy. This is supported by experiments on the yield of electron transfer scavenging of the different excited states by NO_3^-. It has been shown that diffuse forms of the hydrated electron have a higher scavenging yield with NO_3^- than the more localized p-state [29]. Fig. 5 compares scavenging yields of the 400 nm excited state with the previously published results with 800 nm excitations. At low pulse energies (<10% bleach) the scavenging yield is significantly smaller for 1-photon 800 nm excitation (square) which produces the p-state, than the 1-photon 400 nm excitation (circle) which produces the conduction band. For larger pulse energies, the 800 nm data show an increase in scavenging yield which eventually increases to the level of the 400 nm data. Under the large % bleach conditions, scavenging occurs from the 2-photon excited conduction band.

It is interesting that the 800 nm excitation scavenging yields in Fig. 5 exhibit a variation of scavenging yield for % bleach values as low as 25%. The 400 nm scavenging yield, in contrast, does not vary over the entire range of % bleach values that are accessible with the available pulse energy. This behavior can be explained by considering the different probability of excited state absorption for 400 nm vs. 800 nm excitation.

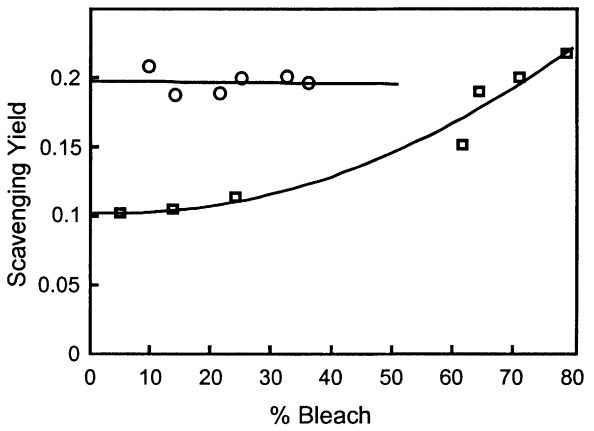

Fig. 5. Scavenging yield of the excited state hydrated electron as a function of the ground state population depleted by the 400 nm (circle) and 800 nm (square) pump pulse in a 0.1 M aqueous $NaNO_3$ solution.

For the 800 nm ~50 fs control pulse excitation experiments the first absorbed photon prepares the p-state. The p-state adiabatically relaxes on the tens of femtosecond time scale to produce a relaxed p-state with (p → CB) absorption band with a significant cross section at 800 nm. An absorption of a second photon by the p → CB band is presumably responsible for all of the following: the 2-photon suppressed geminate recombination, the increased scavenging yield, and the increased time-scale for the relaxation (as in Fig. 3b). In contrast, for 400 nm excitation, the conduction band and its subsequently formed relaxation intermediates, absorb at significantly longer wavelengths at early times than 400 nm. This insures that the 400 nm control pulse experiments are less susceptible to 2-photon effects.

It is important to consider the implications of the result of this Letter on the interpretation of 1-photon absorption spectrum of e_{eq}. As mentioned in Section 1, theory suggests that the main peak in the hydrated electron absorption spectrum is due to the s → p transition, which carries more than 90% of the oscillator strength [17]. At shorter wavelengths a weak s → CB shoulder is predicted [19]. The results herein are indeed highly consistent with this theoretical prediction. However, it is worth considering a closely related, but alternative interpretation. It is possible that the absorption probability at 400 nm is in fact due to the p-state if, the p-state formed by excitation at this wavelength is efficiently converted by a radiationless transition to the conduction band state. In other words it is possible that at 400 nm the sequence of process is as follows.

$$s \overset{400\ nm}{\rightarrow} p \overset{nonradiative}{\rightarrow} CB \tag{2}$$

If this is in fact the source of conduction band electron, essentially all of the intermediate p-state would have to undergo the non-radiative detrapping process since the observed yield of detrapping is close to unity. (Of course, at longer wavelengths such as 800 nm, the p-state does not undergo detrapping.) A detailed investigation of the wavelength dependence of the 1-photon suppressed geminate recombination yield would help determine to what extent Eq. (2) is a factor in the excitation process.

In future papers we will explore the control pulse wavelength dependence of the yield of suppressed geminate recombination in order to determine the threshold for photoinduced detrapping. Such data would also be useful in developing an understanding of the low-lying states of the conduction band. Analogous attempts to study the conduction band of water with multiphoton ionization have been complicated by the optical excitation of localized Rydberg excited states of water and other potential effects such as optical charge transfer between an excited water molecule and a pre-existing electron trap site in water [22,27]. The near unity detrapping yield and

the large observed σ (>35 Å) in the 3-pulse 400 nm control pulse experiment strongly suggests that the 3-pulse technique is a 'cleaner' approach for investigating the spectroscopy and dynamics of the conduction band.

4. Conclusion and summary

Several types of experimental evidence are presented in support of the assignment that the UV portion of the hydrated electron absorption corresponds to an s-state to conduction band transition. The strongest evidence is the observation that 400 nm excitation of an equilibrated hydrated electron induces a >35 Å migration in solution. The migration was monitored by the recently reported 3-pulse suppressed geminate recombination technique [18]. Other evidence that the 400 nm excitation produces a conduction band electron includes scavenging yield measurements [29,30] and high time resolution pump–probe data, which monitors the relaxation of the conduction band electrons. The 3-pulse, 400 nm control pulse experiment described herein is a powerful new tool for exploring the spectroscopy and dynamics of conduction band electron in water.

Acknowledgements

We gratefully acknowledge support of this research by the Basic Energy Sciences Program of the Department of Energy and the Robert A. Welch Foundation. We also thank P.J. Rossky for helpful discussions.

References

[1] P.J. Rossky, J.D. Simon, Nature 370 (1994) 263.
[2] E.J. Hart, M. Anbar, The Hydrated Electron, Wiley, New York, 1970.
[3] A. Mozumder, Fundamentals of Radiation Chemistry, Academic Press, London, 2000.
[4] J.W.T. Spinks, R.J. Woods, An Introduction to Radiation Chemistry, Wiley, New York, 1976.
[5] S.M.A. Pottinger, Radiation Biology: A Textbook: General Consideration of Radiation Damage, Mount Saint Scholastica College, Tape Institute, Atchison, Kansas, 1962.
[6] N.A. Dyson, Radiation Physics with Applications in Medicine and Biology, E. Horwood, New York, 1993.
[7] A. Staib, D. Borgis, J. Chem. Phys. 103 (1995) 2642.
[8] R.B. Barnett, U. Landman, A. Nitzan, J. Chem. Phys. 90 (1989) 4413.
[9] A. Migus, Y. Gauduel, J.L. Martin, A. Antonetti, Phys. Rev. Lett. 58 (1987) 1559.
[10] F.H. Long, H. Lu, K.B. Eisenthal, Phys. Rev. Lett. 64 (1990) 1469.
[11] F.H. Long, H. Lu, X. Shi, K.B. Eisenthal, Chem. Phys. Lett. 185 (1991) 47.
[12] K. Yokoyama, C. Silva, D.H. Son, P.K. Walhout, P.F. Barbara, J. Phys. Chem. A 102 (1998) 6957.
[13] C. Silva, P.K. Walhout, K. Yokoyama, P.F. Barbara, Phys. Rev. Lett. 80 (1998) 1086.
[14] M. Assel, R. Laenen, A. Laubereau, Chem. Phys. Lett. 317 (2000) 13.
[15] J.A. Kloepfer, V.H. Vilchiz, V.A. Lenchenkov, A.C. Germaine, S.E. Bradforth, J. Chem. Phys. 113 (2000) 6288.
[16] V.H. Vilchiz, J.A. Kloepfer, A.C. Germaine, V.A. Lenchenkov, S.E. Bradforth, J. Phys. Chem. A (2000) 1711.
[17] J. Schnitker, K. Motakabbir, P.J. Rossky, R. Friesner, Phys. Rev. Lett. 60 (1988) 456.
[18] P. Kambhampati, D.H. Son, T.W. Kee, P.F. Barbara, J. Phys. Chem. A, submitted.
[19] K.A. Motakabbir, P.J. Rossky, Chem. Phys. 129 (1989) 253.
[20] B.J. Schwartz, P.J. Rossky, J. Chem. Phys. 101 (1994) 6917.
[21] F.J. Webster, J. Schnitker, M.S. Friedriches, R.A. Friesner, P.J. Rossky, Phys. Rev. Lett. 66 (1991) 3172.
[22] M.U. Sander, M.S. Gudiksen, K. Luther, J. Troe, Chem. Phys. 258 (2000) 257.
[23] D.M. Bartels, R.A. Crowell, J. Phys. Chem. 104 (2000) 3349.
[24] K.A. Motakabbir, J. Schnitker, P.J. Rossky, J. Chem. Phys. 97 (1992) 2055.
[25] T. Goulet, J.P. Jay-Gerin, J. Chem. Phys. 96 (1992) 5076.
[26] S.M. Pimblott, J. Phys. Chem. 95 (1991) 6946.
[27] R.A. Crowell, D.M. Bartels, J. Phys. Chem. 100 (1996) 17940.
[28] M. Assel, R. Laenen, A. Aaubereau, J. Chem. Phys. 111 (1999) 6869.
[29] D.H. Son, P. Kambhampati, T.W. Kee, P.F. Barbara, J. Am. Chem. Soc. (2000) submitted.
[30] T.W. Kee, D.H. Son, P. Kambhampati, P.F. Barbara, J. Phys. Chem. (2000) submitted.